

Precipitation of silver nanoparticles in glass by multiple wavelength nanosecond laser irradiation

J.-P. BLONDEAU*, O. VERON

Institut PRISME, Orleans University, 21 rue de Loigny La Bataille, 28000 Chartres, France

The effect of a multiple high power Nd:YAG laser radiation on silver ion-exchanged glasses for coloration application is investigated. Exposure time, laser spot size, energy density and wavelength have been varied in order to modify the size and the distribution of the metallic nanoaggregates which are formed under the laser irradiation. These parameters are directly correlated to the coloration change. Optical absorption spectroscopy has been used to confirm the formation of the nanoaggregates by plasmon resonance apparition and the intensity and the shift of the resonance have been observed with the laser irradiation parameters variation.

(Received June 30, 2009; accepted November 13, 2009)

Keywords: Nanosecond laser, Ionic exchange, Surface plasmon resonance, Silver nano particles

1. Introduction

Metallic nanopowders have been widely studied because they have interesting physical properties which are considerably different from the bulk phase. These nanoscale materials are expected to have many potential applications such as heterogeneous catalysts, surfaces of heat exchangers, memory devices, gas sensors, optical waveguides or optical switches [1–4]. Especially, extensive studies have been conducted on silver nanosized particles owing to their commercial applications for construction of medical tools and appliances and healthcare products [5,6]. Such heterogeneous materials, being composed of metallic nanoclusters in amorphous matrices, are fabricated by a variety of methods. The most successful are low energy ion-beam mixing [7], sol-gel [8], direct metal ion implantation [9], annealing of ion-exchanged glasses in hydrogen atmosphere or evaporation-condensation [10–12]. In recent years, great effort has been taken to the processing of such nano composites using pulsed laser irradiation of ion-exchange glasses. The electric field intensity of a focused laser beam can reach even $100\text{TW}/\text{cm}^2$ in the case of femtosecond lasers. Therefore various microstructures are created when the laser pulse is focused into transparent materials due to multiphoton processes. A number of experimental works with pulsed Nd:YAG laser irradiation concern metal polymer nanostructures, photochromic glasses, optical waveguides which all consist in the ion-exchange process in sodalime glasses [13–16]. In this work we investigate the effect of high power laser irradiation on sodium–silver ion exchanged glasses at room temperature which promotes the formation of silver nanoparticles by diffusion and aggregation. The second harmonic and the fourth harmonic of the Nd:YAG laser at respectively 532nm and 266nm was selected as a light source. Modification of the structure of the dielectric medium is investigated by UV–

Visible absorption measurements. Three principal parameters are varied during our investigations: the immersion time τ , the fluence of the single laser shot E and the number N_b of laser shots which determines the total fluence E_T deposited to the sample. Note that P represents the power density.

2. Preparation of the sodium–silver ion exchange glasses

Soda lime glass slides ($76 \times 25 \times 1\text{ mm}^3$) with a homogeneous composition of 71.67 % SiO_2 14.93 % Na_2O 4.28 % K_2O 5.40 % CaO 3.72 % BaO were prepared by a silver-sodium exchange process and immersed for $\tau = 1$ to 390 minutes in a molten salt bath of molar concentration 10 % AgNO_3 in NaNO_3 at $T = 400^\circ\text{C}$. In these conditions the sodium ions at the glass surface are replaced by silver ions.

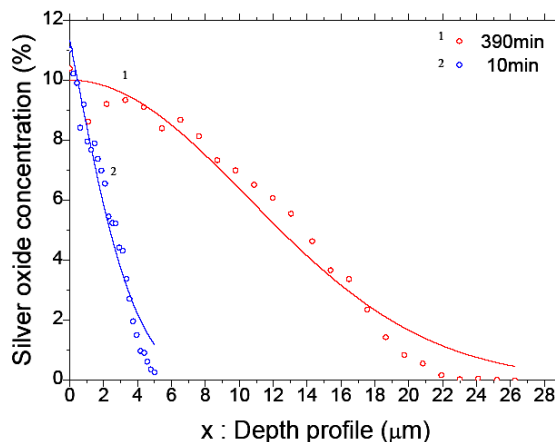


Fig. 1. Silver oxide concentration profile versus the ion exchange depth..

Silver oxide concentrations profiles $c(x, \tau)$ observed by SEM in EDS configuration and have been plotted as a function of ion exchange depth [Dot graph in Fig. 1] and lead to a maximum depth of 25 μm in agreement with the theoretical law [Curves in Fig. 1] of temporal variation (diffusion profile in an infinite medium with a fixed concentration in $x=0$ and constant in time):

$$c(x, \tau) = c_0 \operatorname{erfc}\left(\frac{x}{2\sqrt{D\tau}}\right) \quad (1)$$

with

$$c(x=0; \tau > 0) = c_0 \quad ; \quad c(x > 0; \tau = 0) = 0 \quad \text{and} \quad \left.\frac{\partial c}{\partial x}\right|_{x \rightarrow \infty, \tau > 0} = 0 \quad (2)$$

In our case, τ corresponds to the immersion time, and the silver diffusion coefficient D in soda lime glass depends on the bath temperature T according to the Arrhenius law.

$$D = D_0 e^{-\frac{E_a}{k_B T}} \quad (3)$$

where E_a is activation energy, D_0 is the pre-exponential factor and k_B is the Boltzmann constant.

The diffusion coefficient plotted in Fig.2 is decreasing until one hour before reaching a steady state when all the sodium sites are replaced by silver near the glass surface.

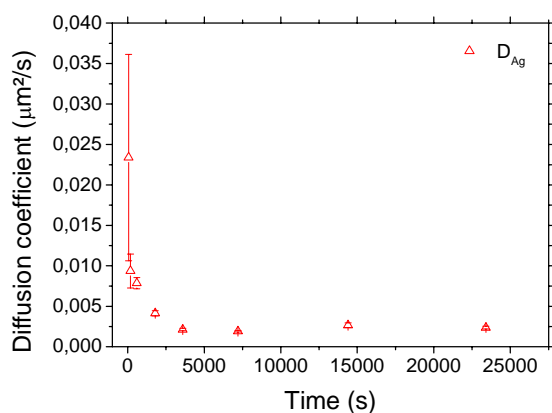


Fig. 2. Silver diffusion coefficient versus time.

The optical absorption spectra in the range of 250–700nm of the ion-exchange samples for different times of dumping τ are plotted in Fig. 3. The absorption of the prepared glasses increases significantly in the blue region due to the introduction of silver ions and to the formation of Ag-O bonds. The atomic silver and hole trap center at non-bridging oxygen (NBO) near Ag^+ ions have, respectively, absorption wavelengths of approximately 240 and 305nm [17,18] that induces the high increase of optical absorption spectra below 400nm. For longer times

we note a significant growth of absorption around 400nm correlated to the formation of silver nano aggregates associated to a silver plasmon resonance appearance.

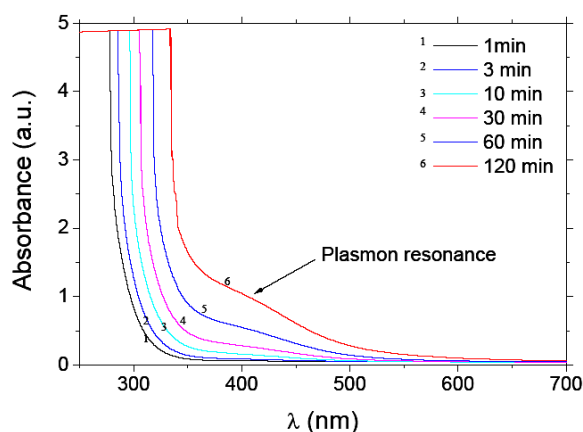
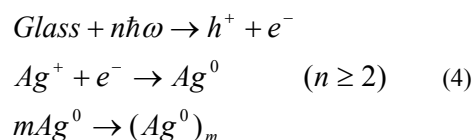


Fig. 3. UV-Visible spectra of samples exchanged in 10% AgNO_3 - NaNO_3 at 400°C for various times.

3. Precipitation of Ag nanoparticles by laser irradiation

The ion-exchange glasses were irradiated by the second and fourth harmonic ($\lambda=532$ photon energy 2.33 eV and 266nm photon energy 4.66 eV) of the pulsed Nd:YAG laser. The laser delivered pulses of energy up to 150mJ at 1064nm of about 4ns duration, at a repetition rate of 10Hz and of the Gaussian cross-sectional area. At 532nm the beam is either directly injected through the glass sample with an energy density E of 0.55J/cm² and a 12.6mm² spot surface or focused through a 50cm focal lens an energy density of 1.6J/cm² and a 4mm² spot surface. At 266 nm the beam is injected through the glass sample with an energy density of 0.12J/cm² and a 12.6mm² spot surface. The increasing number of shots typically range from 10 to 400 allow to vary the total deposited energy on the ion exchange sample.

In every case, the formation of silver nanoparticles can be described as follows:



where n is the number of photons; h is a hole; e^- is an electron; and m is the number of Ag atoms forming the nanoparticle.

Laser irradiation induces a wide absorption band centred at about 425nm which is assigned to plasmon band. This band results from the light absorption by Ag nanoparticles and direct excitation of the surface plasmon waves [19,20].

Fig. 4, Fig.6 and Fig.7 show the evolution of the absorption spectra during the irradiation process (the

growth of the total fluence E_T is due to the increasing of the number of shots from 10 to 200) for a fixed exchange time $\tau=60\text{min}$ respectively for $\lambda=532\text{nm}$ ($E=1.6\text{J}/\text{cm}^2$ and $E=0.55\text{J}/\text{cm}^2$) and $\lambda=266\text{nm}$, $E=0.12\text{J}/\text{cm}^2$. The coloration change from yellow to brown is visible in the Fig.5 and correlated to the increasing number of shots.

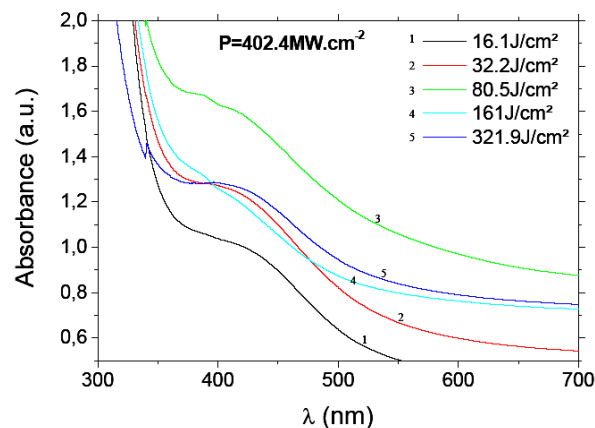


Fig. 4. Silver exchanged sample for $\tau=60\text{min}$ after $\lambda=532\text{nm}$ irradiation with pulse energy $\approx 64\text{mJ}$, $E=1.6\text{J}/\text{cm}^2$ by shot (10 to 200 shots).

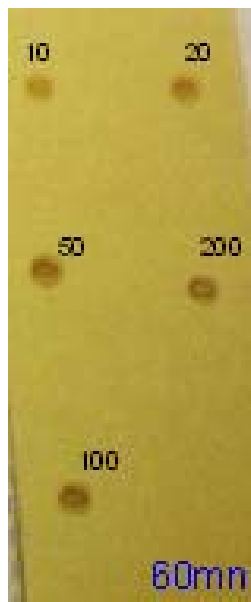


Fig.5. Silver exchange sample after YAG nano second laser irradiation at 532nm ; $E=1.6\text{J}/\text{cm}^2$ for 10 to 200 shots.

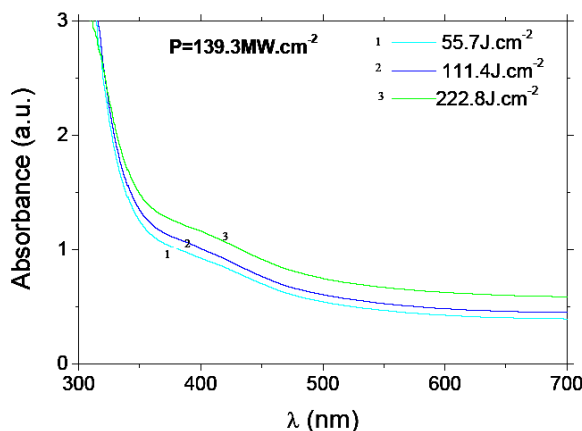


Fig.6. Silver exchanged sample at $\tau=60\text{min}$ after $\lambda=532\text{nm}$ irradiation with pulse energy $\approx 70\text{mJ}$, $E=0.55\text{J}/\text{cm}^2$ by shot.

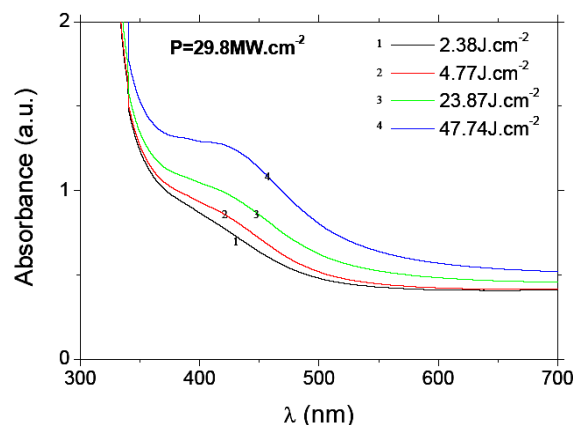


Fig.7. Silver exchanged sample at $\tau=60\text{min}$ after $\lambda=266\text{nm}$ irradiation with pulse energy $\approx 15\text{mJ}$, $E=0.12\text{J}/\text{cm}^2$ by shot.

We observe an increase of the absorption intensity for total fluence under $E_T=80\text{J}/\text{cm}^2$ (see Fig.4 for $\lambda=532\text{nm}$ and $E=1.6\text{J}/\text{cm}^2$) and a decrease above which is correlated to a particle growth and a dissolution mechanism for the highest energy.

According to a lorentzian fit in Fig. 8 the evolution of the maximum resonance wavelength is plotted in Fig.9 for all the exchange times and show a blue shift trend with increasing energy for all cases which is correlated to a particle dissolution. The red-shift for the last exchange time could be justified by the following reasons, a matrix effect due to ablation of the glass and the difficulty to fit the curve because intensity becomes lower.

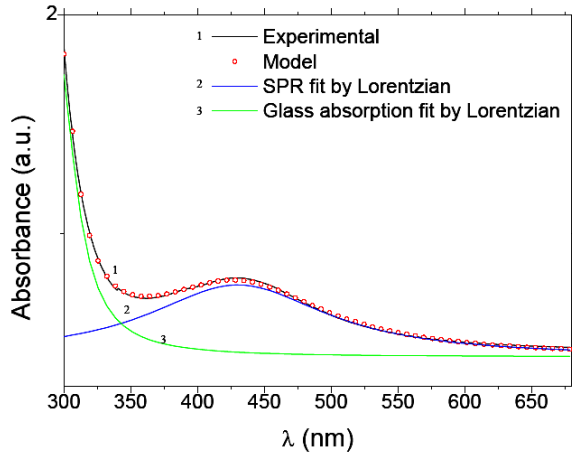


Fig. 8. Example of lorentzian fit of the absorption curve.

This trend is also observed in Fig.6 for $\lambda=532\text{nm}$ and $E=0.55\text{J/cm}^2$ and Fig.10 where the increasing energy lead to a blue shift of the maximum resonance wavelength.

For $\lambda=266\text{nm}$ and $E=0.12\text{J/cm}^2$ in Fig.7 and Fig.11 we observe a red shift of the maximum resonance wavelength which means that we are only in a growth regime without dissolution.

This wavelength is in the absorption window of the glass and metal (Silver interband transition located at 318nm) and far from the plasmon resonance of silver which is around 410nm and lead to a limitation of the thermal phenomena. The plasmon resonance apparition occurs for lower energy when the sample is irradiated by an UV beam (266nm) that means that the irradiation mechanism is more efficient.

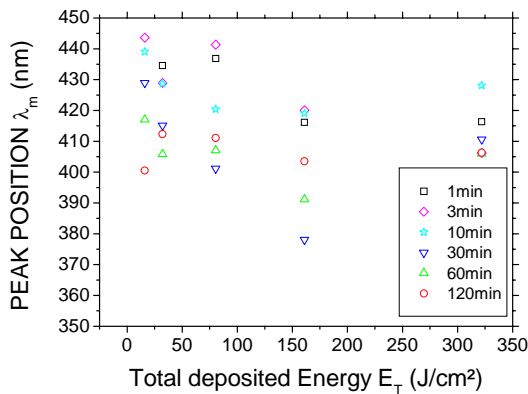


Fig. 9. Peak position evolution for YAG irradiation at $\lambda=532\text{nm}$, pulse energy $\approx 64\text{mJ}$, spot surface $\approx 4\text{mm}^2$, $E=1.61\text{J/cm}^2$, $P=402.4\text{MW/cm}^2$.

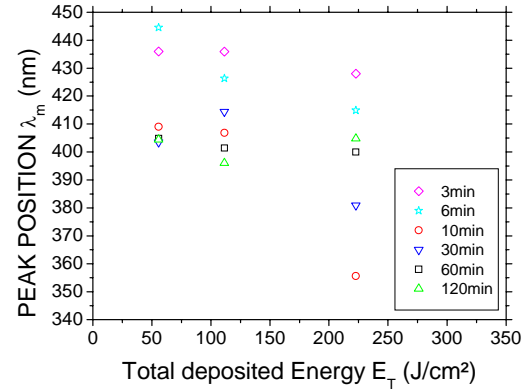


Fig.10. Peak position evolution for YAG irradiation at $\lambda=532\text{nm}$, pulse energy $\approx 70\text{mJ}$, spot surface $\approx 12.6\text{mm}^2$, $E=0.55\text{J/cm}^2$, $P=139.3\text{MW/cm}^2$.

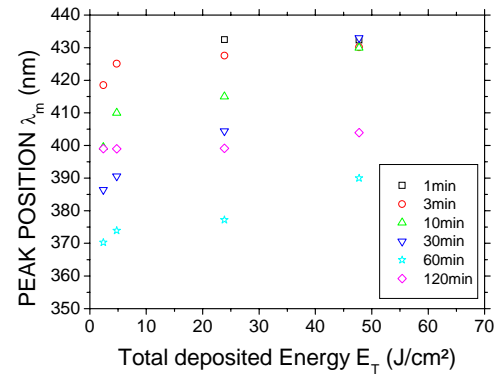


Fig. 11. Peak position evolution for YAG irradiation at $\lambda=266\text{nm}$, pulse energy $\approx 15\text{mJ}$, spot surface $\approx 12.6\text{mm}^2$, $E=0.12\text{J/cm}^2$, $P=29.8\text{MW/cm}^2$.

From a theoretical point of view the absorption peaks are due to the surface plasmon resonance of silver cluster. The particle size distribution is dominated by a mean size R with volume fraction N which gives the absorption intensity as a function of the absorption cross section σ .

$$A(\lambda, R) = N \cdot \sigma(\lambda, R) \cdot l \quad (5)$$

where N is the particle density in the matrix, and l is the thickness of the sample.

According to Drude model [21], absorption cross-section $\sigma(\lambda, R)$ of silver nano-clusters at wavelength λ varies with particle mean size R as:

$$\sigma(\lambda, R) = \frac{18 \pi V n^3}{\lambda} \frac{\varepsilon_2}{(\varepsilon_1 + 2n^2)^2 + \varepsilon_2^2} \quad [\text{cm}^{-1}] \quad (6)$$

where the metal dielectric function is given by

$$\varepsilon_{Drude}(\omega) = 1 - \frac{\omega_p^2}{\omega^2 + i\Gamma_{Bulk}(R)\omega} \equiv \varepsilon_{1,Drude}(\omega) + i\varepsilon_{2,Drude}(\omega) \quad (7)$$

with

$$\begin{cases} \varepsilon_{1,Drude}(\omega) = 1 - \frac{\omega_p^2}{\omega^2 + \Gamma_{Bulk}^2} \\ \varepsilon_{2,Drude}(\omega) = \frac{\omega_p^2 \cdot \Gamma_{Bulk}}{\omega(\omega^2 + \Gamma_{Bulk}^2)} \end{cases} \quad (8)$$

and

$$\omega = \frac{2\pi c}{\lambda} \quad (9)$$

V is the particle volume, linked to its size R ; ω , the angular frequency in rad/s; ω_p , the plasmon resonance frequency; n is the refractive index of the matrix; and Γ_{Bulk} is the effective damping parameter for the free electrons in the bulk metal.

Taking into account the interband transitions of the metal in the expression of Γ , and the effect of reduction of electron mean free path when confined in particles whose size is smaller than the bulk mean free path ($\approx 52\text{nm}$ for pure silver at 273 K [22]), we have

$$\begin{cases} \varepsilon_1(\omega, R) = \varepsilon_{1Inter} + \varepsilon_{1Drude} = \varepsilon_{1Inter} + 1 - \frac{\omega_p^2}{\omega^2 + \Gamma(\omega, R)^2} \\ \varepsilon_2(\omega, R) = \varepsilon_{2Inter} + \varepsilon_{2Drude} = \varepsilon_{2Inter} + \frac{\omega_p^2 \cdot \Gamma}{\omega(\omega^2 + \Gamma(\omega, R)^2)} \end{cases} \quad (10)$$

with

$$\Gamma(R) = \Gamma_{Bulk} + A \frac{V_f}{R} \quad (11)$$

ε_1 and ε_2 are the real and imaginary parts of the dielectric function of the nanoparticles; ε_{1Inter} and ε_{2Inter} are the real and imaginary part of the frequency dependent dielectric function of bulk silver due to the inter-band transitions; A is a model-depending parameter ($A = 2.00$ [23] \div 0.25 [24]);

Γ_{Bulk} is the absorption coefficient of the plasmon electron and the second term in the expression of Γ is used to introduce a size-dependent term in the damping frequency with the nano-particle size R ; V_f is the Fermi's velocity of electrons in bulk silver ($V_f = 1.39 \times 10^8 \text{ cm.s}^{-1}$ in the case of silver) [21].

4. Discussion

According to the MIE theory [25] the appearance of the plasmon resonance band around 420 nm suggests that

the pulsed laser processing of glasses leads to the formation of silver nanoparticles. The blue shift observed for irradiation at 532nm in the absorption coefficient band certainly results in a decrease in the mean size of these nanoparticles with the increasing energy or can be attributed to a decrease in the filling factor of the glass by the formation of the nanoparticles; in fact a decrease of the fraction of silver which leads to the formation of the nanoparticles.

The increasing energy leads first to the growth of particles and in a second time to a size reduction. It can be attributed to dissolution effects in agreement with the absorption curves by a move of the resonance towards the shorter wavelength.

At 266nm the irradiation only leads to a plasmon resonance red shift and a particle growth.

The power by pulse is an important parameter for the space-selective precipitation of silver nanoparticles in glass. Its principal effect is to locally warm up the sample to promote the reduction of Ag^+ ions to silver atoms and the growth of the silver nanoparticle.

The various parameters immersion time τ , power by shot P , and total deposited energy E_T from the number of shots N_b and available laser energy, are thus directly correlated and must be precisely adjust not to destroy the sample by surface breakdown and laser induced plasma.

5. Conclusions and trend

The laser irradiation of silver ion-exchanged glasses is a relatively new and original method to generate a space-selective precipitation and aggregation of metal nanoparticles inside a vitreous matrix, to modify their optical characteristics and allow a process control.

The silver nanoparticles produce the absorption bands with maximum at about 420nm which are attributed to the surface plasmon resonance (SPR).

The absorption spectra change with the immersion time but also with the laser intensity, fluence, and with the number of the laser shots due to the heat treatment effects. Modifications of the extinction spectra are related to variations of the damping constant Γ , predominantly with the size and the shape of the nanoparticles.

When the samples are irradiated at 266nm the SPR apparition is obtained for lower energies than at 532nm due to the interband transition of the metal which occurs in the UV region (310nm for silver) and to the glass absorption, and a limitation of the thermal effects.

With increasing the laser intensity and the irradiation time, the colour of the irradiated area has changed from yellow to brown.

The linear optical properties of nano composites containing silver nanoparticles embedded in a host dielectric medium are due to the excitation of SPR. The SPR is responsible for the enhancement of the local electromagnetic field in the particles, which amplifies their non linear properties as compared to those of bulk metal. Thus it is advisable to study such materials in terms of

their nonlinear properties and to correlate them with their morphologic parameters.

Acknowledgements

Thanks to Quantel Society for helpful investigation on our samples.

References

- [1] G.C. Bond, Surf. Sci. **156**(2), 966 (1985).
- [2] G. Mitrikas, Y. Deligiannakis, C.C. Trapalis, N. Boukos, G. Kordas, J. Sol–Gel Sci. Technol. **13**, 503 (1998).
- [3] P. Faccio, Di. Trapani, E. Borsella, F. Gonella, P. Mazzoldi, A.M. Malvezzi, Europhys. Lett. **43**, 213 (1998).
- [4] S. A. Maier, H. A. Atwater, J. Appl. Phys. **98**, 011101 (2005).
- [5] M. Kokkoris, C. C. Trapalis, S. Kossionides, R. Vlastou, B. Nsouli, R. Grotzschel, G. Kordas, Th. Paradellis, Nucl. Instrum. Methods Phys. Res. B **188**, 67 (2002).
- [6] M. Kawashita, S. Tsuneyama, F. Miyaji, T. Kokubo, H. Kozuka, K. Yamamoto, Biomaterials **21**, 393 (2000).
- [7] P. Gangopadhyay, R. Kesavamoorthy, K. G. M. Nair, R. Dhandapani, J. Appl. Phys. **88**, 4975 (2000).
- [8] M. Epifani, C. Giannini, L. Tapfer, L. Vasanelli, J. Am. Ceram. Soc. **83**, 2385 (2000).
- [9] A. Miotello, G. DeMarchi, G. Mattei, P. Mazzoldi, A. Quaranta, Appl. Phys. **A70**, 415 (2000).
- [10] F. Catan, «Elaboration et Caractérisation de Nanoparticules Métalliques par voie physicochimique, Application à la coloration des verres » Ph.D.Thesis, Orleans University, France, 31/01/2007.
- [11] F. Catan, D. De Sousa Meneses, J. P. Blondeau, L. Allam, J. Non-Cryst. Solids **354**, 1026 (2008).
- [12] J. P. Blondeau, F. Catan, C. Andreazza-Vignolle, N. Sbai, Plasmonics **3**, 65 (2008).
- [13] G. deMarchi, F. Caccavale, F. Gonella, G. Mattei, P. Mazzoldi, G. Battaglin, A. Quaranta, Appl. Phys. **A63**, 403 (1996).
- [14] Zeng Hui-Dan, Qiu Jian-Rong, Jiang Xiong-Wei, Qu Shi-Liang, Zhu Cong-Shan and Gan Fu-Xi, Phys.Lett. **20**(6), 932 (2003).
- [15] H. Zeng, C. Zhao, J. Qiu, Y. Yang, G. Chen, J. Crystal Growth **300**, 519 (2007).
- [16] J. Zhang, W. Dong, J. Sheng, J. Zheng, J. Li, L. Qiao, L. Jiang, J. Crystal Growth **310**, 234 (2008).
- [17] M. Tashiro, N. Soga: Kogyo Kagaku Zasshi **65**, 342 (1962) [in. Japanese].
- [18] J. Qiu, M. Shirai, T. Nakaya, J. Si, X. Jiang, C. Zhu, K. Hirao, Appl. Phys. Lett. **81**, 3040 (2002).
- [19] Kreibig, Uwe, Vollmer, Michael, Optical Properties of Metal Clusters, Springer, Berlin, 1995.
- [20] F. Hache, D. Ricard, C. Flytzanis, J. Opt. Soc. Am. B, Opt. Phys. **3**, 1647 (1986).
- [21] J. Zhang, W. Dong, L. Qiao, J. Li, J. Zheng, J. Sheng, J. Crystal Growth **305**, 278 (2007).
- [22] J. Sheng, J. Zheng, J. Zhang, C. Zhou, L. Jiang, Phys. B Condens. Matter **387**(1), 32 (2007).
- [23] A. Pinchuk, U. Kreibig, A. Hilger, Surf. Sci. **557**, 269 (2004).
- [24] M. Rashidi-Huyeh, B. Palpant, J. Appl. Phys. **96**(8), 4475 (2004).
- [25] C. F. Bohren, D.R. Huffman, Absorption and Scattering of Light by Small Particles, Wiley Science Paperback Series, 1983.

*Corresponding author:

jean-philippe.blondeau@univ-orleans.fr